ZARTS: On Zero-order Optimization for Neural Architecture Search

Anonymous Author(s)
Affiliation
Address
email

Abstract

Differentiable architecture search (DARTS) has been a popular one-shot paradigm for NAS due to its high efficiency. It introduces trainable architecture parameters to represent the importance of candidate operations and proposes first/second-order approximation to estimate their gradients, making it possible to solve NAS by gradient descent algorithm. However, our in-depth empirical results show that the approximation often distorts the loss landscape, leading to the biased objective to optimize and, in turn, inaccurate gradient estimation for architecture parameters. This work turns to zero-order optimization and proposes a novel NAS scheme, called ZARTS, to search without enforcing the above approximation. Specifically, three representative zero-order optimization methods are introduced: RS, MGS, and GLD, among which MGS performs best by balancing the accuracy and speed. Moreover, we explore the connections between RS/MGS and gradient descent algorithm and show that our ZARTS can be seen as a robust gradient-free counterpart to DARTS. Extensive experiments on multiple datasets and search spaces show the remarkable performance of our method. In particular, results on 12 benchmarks verify the outstanding robustness of ZARTS, where the performance of DARTS collapses due to its known instability issue. Also, we search on the search space of DARTS to compare with peer methods, and our discovered architecture achieves 97.54% accuracy on CIFAR-10 and 75.7% top-1 accuracy on ImageNet. Finally, we combine our ZARTS with three orthogonal variants of DARTS for faster search speed and better performance.

1 Introduction

Despite their success, neural networks are still designed mainly by humans [27, 14, 15]. It remains open to search for efficient architectures automatically. The problem of neural architecture search (NAS) has attracted wide attention, which can be modeled as bi-level optimization for network architectures and operation weights. One-shot NAS [1] is a popular search framework that regards neural architectures as directed acyclic graphs (DAG) and constructs a supernet with all possible connections and operations in the search space. DARTS [20] further introduces trainable architecture parameters to represent the importance of candidate operations, which are alternately trained by SGD optimizer along with network weights. It proposes a first-order approximation to estimate the gradients of architecture parameters, which is biased and may lead to the severe instability issue shown by [3]. Other works [38, 6] point out that architecture parameters will converge to a sharp local minimum resulting in the instability issue, so they introduce extra regularization items making architecture parameters converge to a flat local minimum.

In this paper, we empirically show that the first-order approximation of optimal network weights sharpens the loss landscape and results in the instability issue of DARTS. It also shifts the global minimum, misleading the training of architecture parameters. To this end, we discard such approximation

Submitted to 36th Conference on Neural Information Processing Systems (NeurIPS 2022). Do not distribute.

and turn to zero-order optimization algorithms, which can run without the requirement that the search loss is differentiable w.r.t. architecture parameters. Specifically, we introduce a novel NAS scheme named ZARTS, which outperforms DARTS by a large margin and can discover efficient architectures stably on multiple public benchmarks. This paper sheds light on the frontier of NAS by:

1) Establishing zero-order based robust paradigm to solve bi-level optimization for NAS. Differentiable architecture search has been a well-developed area [20, 34, 31] which solves the bi-level optimization of NAS by gradient descent algorithms. However, this paradigm suffers from the instability issue during search since biased approximation for optimal network weights distorts the loss landscape, as shown in Fig. 1 (a) and (b). To this end, we propose a flexible zero-order optimization NAS framework to solve the bi-level optimization problem, which is compatible with multiple potential gradient-free algorithms in the literature.

2) Uncovering the connection between zero-order architecture search and DARTS. This work introduces three representative zero-order optimization algorithms without enforcing the unverified differentiability assumption for search loss w.r.t. architecture parameters. We reveal the connections between the zero-order algorithms and gradient descent algorithm, showing that two implementations of ZARTS can be seen as gradient-free counterparts to DARTS, being more stable and robust.

3) Strong empirical performance and robustness. Experiments on four datasets and five search spaces show that, unlike DARTS that suffers the severe instability issue [38, 3], ZARTS can stably discover effective architectures on various benchmarks. In particular, the searched architecture achieves 75.7% top-1 accuracy on ImageNet, outperforming DARTS and most of its variants. Also, our ZARTS can be further improved by combining with orthogonal DARTS variants, achieving 97.81% on CIFAR-10 after searching in 0.5 GPU-day.

2 Related Work

One-shot Neural Architecture Search. [1] construct a supernet so that all candidate architectures can be seen as its sub-graph. DARTS [20] introduces architecture parameters to represent the importance of operations in the supernet and update them by gradient descent algorithm. Some works [34, 31, 10] reduce the memory requirement of DARTS in the search process. Other works [38, 6] point out the instability issue of DARTS, i.e., skip-connection gradually dominates the normal cells, leading to performance collapse during the search stage.

Bi-level Optimization for NAS. NAS can be modeled as a bi-level optimization for architecture parameters and network weights. DARTS [20] proposes the first/second-order approximations to estimate gradients of architecture parameters so that they can be trained by gradient descent. However, we show that such approximation will distort the loss landscape and mislead the training of architecture parameters. Amended-DARTS [3] derives an analytic formula of the gradients w.r.t. architecture parameters that require the inverse of Hessian matrix of network weights, which is even unfeasible to compute. This work discards the approximation in DARTS and attempts to solve the bi-level optimization by gradient-free algorithms.

Zero-order Optimization. Unlike gradient-based optimization methods that require the objective differentiable w.r.t. the parameters, zero-order optimization can train parameters when the gradient is unavailable or difficult to obtain, which has been widely used in adversarial robustness for neural networks [5, 16], meta learning [28], and transfer learning [29]. [22] aim at AutoML and utilize zero-order optimization to discover optimal configurations for ML pipelines. In this work (to our best knowledge), we make the first attempt to apply zero-order optimization to NAS and experiment with multiple algorithms, from vanilla random search [11] to more advanced and effective direct search [12], showing its great superiority against gradient-based methods.

3 Bi-level Optimization in DARTS

Following one-shot NAS [1], DARTS constructs a supernet stacked by normal cells and reduction cells. Cells in the supernet are denoted by directed acyclic graphs (DAG) with N nodes $\{x_i\}_{i=1}^{N}$, which represents latent feature maps. Each edge $e_{i,j}$ contains multiple operations $\{o_{i,j}, o \in \mathcal{O}\}$, whose importance is represented by architecture parameters $\boldsymbol{\alpha}_{i,j}^{o}$. Therefore, NAS can be modeled as a bi-level optimization problem by alternately updating the operation weights $\boldsymbol{\omega}$ (parameters within

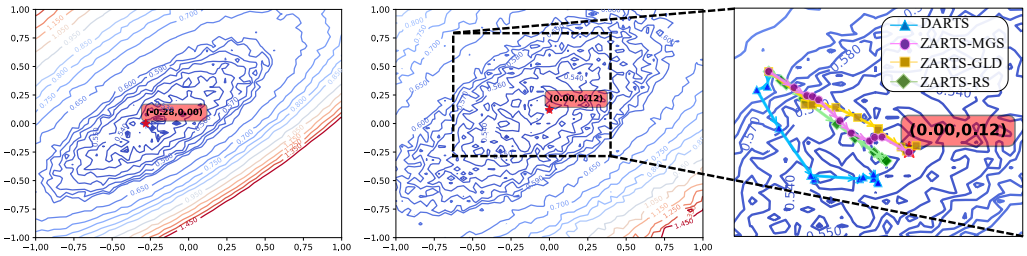

(a) Landscape w.r.t. α with ω^*_{1st} (b) Landscape w.r.t. α with ω^* (c) Tracks of optimization path

Figure 1: Loss landscapes w.r.t. architecture parameters $\boldsymbol{\alpha}$ where the red star indicates the global minimum. (a) the landscape with $\boldsymbol{\omega}^*_{1st}$. (b) the landscape with $\boldsymbol{\omega}^*$, which is obtained by training $\boldsymbol{\omega}$ for 10 iterations. To fairly compare the landscapes in (a) and (b), we utilize the same model and candidate $\boldsymbol{\alpha}$ points. We observe that the first-order approximation sharpens the landscape. (c) displays the tracks of optimization path of DARTS and ZARTS. Starting at the same initial point, ZARTS converges to the global minimum, but DARTS fails.

candidate operations on each edge) and the architecture parameters $\boldsymbol{\alpha}$:

$$\min_{\boldsymbol{\alpha}} \quad \mathcal{L}_{val}(\boldsymbol{\omega}^*(\boldsymbol{\alpha}), \boldsymbol{\alpha}), \quad \text{s.t.} \;\; \boldsymbol{\omega}^*(\boldsymbol{\alpha}) = \arg\min_{\boldsymbol{\omega}} \mathcal{L}_{train}(\boldsymbol{\omega}, \boldsymbol{\alpha}). \tag{1}$$

3.1 Fundamental Limitations in DARTS

By enforcing an unverified (and in fact difficult to verify) assumption that the search loss $\mathcal{L}_{val}(\boldsymbol{\omega}^*(\boldsymbol{\alpha}), \boldsymbol{\alpha})$ is differentiable w.r.t. $\boldsymbol{\alpha}$, DARTS [20] proposes a second-order approximation for the optimal weights $\boldsymbol{\omega}^*(\boldsymbol{\alpha})$ by applying one-step gradient descent:

$$\boldsymbol{\omega}^*(\boldsymbol{\alpha}) \approx \boldsymbol{\omega}^*_{2nd}(\boldsymbol{\alpha}) = \boldsymbol{\omega} - \xi \nabla_{\boldsymbol{\omega}} \mathcal{L}_{train}(\boldsymbol{\omega}, \boldsymbol{\alpha}) = \boldsymbol{\omega}', \tag{2}$$

where ξ is the learning rate to update network weights. Thus the gradient of the loss w.r.t. $\boldsymbol{\alpha}$, $\nabla_{\boldsymbol{\alpha}} \mathcal{L}_{val}(\boldsymbol{\omega}^*(\boldsymbol{\alpha}), \boldsymbol{\alpha})$, can be computed by the chain rule: $\nabla_{\boldsymbol{\alpha}} \mathcal{L}_{val}(\boldsymbol{\omega}^*(\boldsymbol{\alpha}), \boldsymbol{\alpha}) \approx \nabla_{\boldsymbol{\alpha}} \mathcal{L}_{val}(\boldsymbol{\omega}', \boldsymbol{\alpha}) - \xi \nabla^2_{\boldsymbol{\alpha},\boldsymbol{\omega}} \mathcal{L}_{train}(\boldsymbol{\omega}, \boldsymbol{\alpha}) \nabla_{\boldsymbol{\omega}'} \mathcal{L}_{val}(\boldsymbol{\omega}', \boldsymbol{\alpha})$. Nevertheless, the second-order partial derivative is hard to compute, so the authors adopt the difference method, which is proved in the appendix.

To further reduce the computational cost, first-order approximation is introduced by assuming $\boldsymbol{\omega}^*(\boldsymbol{\alpha})$ being independent of $\boldsymbol{\alpha}$, as shown in Eq. 3, which is much faster and widely used in many variants of DARTS [7, 31, 38].

$$\boldsymbol{\omega}^*(\boldsymbol{\alpha}) \approx \boldsymbol{\omega}^*_{1st}(\boldsymbol{\alpha}) = w. \tag{3}$$

The gradient is then simplified as: $\nabla_{\boldsymbol{\alpha}} \mathcal{L}_{val}(\boldsymbol{\omega}^*(\boldsymbol{\alpha}), \boldsymbol{\alpha}) \approx \nabla_{\boldsymbol{\alpha}} \mathcal{L}_{val}(\boldsymbol{\omega}, \boldsymbol{\alpha})$, which exacerbates the estimation bias. Reexamining the definition of $\boldsymbol{\omega}^*(\boldsymbol{\alpha})$ in Eq. 1, one would note that it is intractable to derive a mathematical expression for $\boldsymbol{\omega}^*(\boldsymbol{\alpha})$, making $\mathcal{L}_{val}(\boldsymbol{\omega}^*(\boldsymbol{\alpha}), \boldsymbol{\alpha})$ even non-differentiable w.r.t. $\boldsymbol{\alpha}$. Yet DARTS has to compromise with such approximations as Eq. 2 and Eq. 3 so that differentiability is established and SGD can be applied. However, such sketchy estimation of optimal operation weights can distort the loss landscape w.r.t. architecture parameters and thus mislead the search procedure, which is shown in Fig. 1 and analyzed in the next section.

3.2 Distorted Landscape and Biased Optimization

Fig. 1 illustrates the loss landscape with perturbations on architecture parameters $\boldsymbol{\alpha}$, showing how different approximations of $\boldsymbol{\omega}^*$ affect the search process. We train a supernet for 50 epochs and randomly select two orthonormal vectors as the directions to perturb $\boldsymbol{\alpha}$. The same group of perturbation directions is used to draw landscapes in Fig. 1(a) and (b) for a fair comparison. Fig. 1(a) shows the loss landscape with the first-order approximation in DARTS, $\boldsymbol{\omega}^*_{1st}(\boldsymbol{\alpha}) = \boldsymbol{\omega}$, while Fig. 1(b) shows the loss landscape with more accurate $\boldsymbol{\omega}^*(\boldsymbol{\alpha})$, which is obtained by fine-tuning the network weights $\boldsymbol{\omega}$ for 10 iterations for each $\boldsymbol{\alpha}$. Landscapes (contours) are plotted by evaluating $\mathcal{L}$ at grid points ranging from -1 to 1 at an interval of 0.02 in both directions. Global minima are marked with stars on the landscapes, from which we have two observations: 1) The approximation $\boldsymbol{\omega}^*_{1st}(\boldsymbol{\alpha}) = \boldsymbol{\omega}$ shifts the global minimum and sharpens the landscape [1], which is the representative characteristic of

[1] A "sharp" landscape has denser contours than a "flat" one.

Algorithm 1 ZARTS: Zero-order Optimization Framework for Architecture Search

Hyper-parameters: Operation weights $\boldsymbol{\omega}$, architecture parameters $\boldsymbol{\alpha}$, sampling number N, iteration number M, update estimation function $\phi(\cdot)$.

repeat

  Sample candidates: $\{\mathbf{u}_i\}_{i=1}^N$, and get $\boldsymbol{\alpha}_i^{\pm} = \boldsymbol{\alpha} \pm \mathbf{u}_i$. Estimate optimal operation weights $\boldsymbol{\omega}^*(\boldsymbol{\alpha}_i^{\pm})$ by descending $\nabla_{\boldsymbol{\omega}} \mathcal{L}_{train}(\boldsymbol{\omega}, \boldsymbol{\alpha}_i^{\pm})$ for M iterations;

  Get update direction: $\mathbf{u}^* = \phi\left(\{\mathbf{u}_i, \boldsymbol{\omega}^*(\boldsymbol{\alpha}_i^{\pm})\}_{i=1}^N\right)$

  Update architecture parameters: $\boldsymbol{\alpha} \leftarrow \boldsymbol{\alpha} + \mathbf{u}^*$;

until Converged

* The sampling strategies and update estimation functions $\phi(\cdot)$ for three different zero-order optimization algorithms are detailed in Table 1.

instability issue as pointed out by [38]. 2) Accurate estimation for $\boldsymbol{\omega}^*$ leads to a flatter landscape, indicating that the instability issue can be alleviated. Moreover, we display the landscape with second-order approximation $\boldsymbol{\omega}_{2nd}^*$ in the appendix, which is also sharp but slightly flatter than Fig. 1 (a). Consequently, we discard the first/second-order approximation in DARTS and instead use more accurate $\boldsymbol{\omega}^*$ coordinated with zero-order optimization.

Fig. 1 (c) shows the optimization paths of DARTS and three methods of ZARTS, illustrating how the approximation in DARTS affects the search process. Starting from the same randomly generated position, we update architecture parameters $\boldsymbol{\alpha}$ for 10 iterations by DARTS and ZARTS and draw the tracks of the optimization path. ZARTS can gradually converge to the global minimum, while DARTS converges to an incorrect point.

4 Zero-order Optimization for NAS

This paper goes beyond the 1st/2nd-order approximation in DARTS and proposes to train architecture parameters $\boldsymbol{\alpha}$ by zero-order optimization, allowing for more accurate estimation for $\boldsymbol{\omega}^*(\boldsymbol{\alpha})$. Alg. 1 outlines the generic form of our ZARTS framework. We adopt three representative techniques: a vanilla zero-order optimizer, random search (RS) [21], and two advanced algorithms: Maximum-likelihood Guided Parameter Search (MGS) [32] and GradientLess Descent (GLD) [12], presented in Sec. 4.1, 4.2, 4.3 as preliminaries. Further, we theoretically establish the connection between ZARTS and DARTS, showing that ZARTS with RS and MGS optimizer can be seen as an expansion of DARTS. In the following, we denote $\mathcal{L}(\boldsymbol{\alpha}) \triangleq \mathcal{L}_{val}(\boldsymbol{\omega}^*(\boldsymbol{\alpha}), \boldsymbol{\alpha})$ as the objective w.r.t. architecture parameters $\boldsymbol{\alpha} \in \mathbb{R}^d$ (Eq. 1), and $\mathcal{L}(\boldsymbol{\alpha} + \mathbf{u}) \triangleq \mathcal{L}_{val}(\boldsymbol{\omega}^*(\boldsymbol{\alpha} + \mathbf{u}), \boldsymbol{\alpha} + \mathbf{u})$, where $\mathbf{u}$ is the update for $\boldsymbol{\alpha}$.

4.1 Optimizer I: ZARTS-RS

Zero-order optimizers have no access to gradient information and construct gradient estimators via zero-order information, typically, the function evaluation. As discussed in [21], gradient estimation techniques can be categorized into different types based on the required number of function evaluations. We adopt *Multi-point estimator*, shown in Table 1, as a baseline of our ZARTS:

$$\hat{\nabla}_{\boldsymbol{\alpha}} \mathcal{L}(\boldsymbol{\alpha}) := \frac{\varphi(d)}{2\mu N} \sum_{i=1}^{N} \left[\mathcal{L}(\boldsymbol{\alpha} + \mu \mathbf{u}_i) - \mathcal{L}(\boldsymbol{\alpha} - \mu \mathbf{u}_i)\right] \mathbf{u}_i. \tag{4}$$

4.2 Optimizer II: ZARTS-MGS

Maximum-likelihood guided parameter search (MGS) is an advanced zero-order optimization algorithm for machine translation [32]. We make the attempt to apply it to the NAS task. We first define a distribution for the update of architecture parameters, $\mathbf{u}$, as follows:

$$p(\mathbf{u}|\boldsymbol{\alpha}) = \frac{\widetilde{p}(\mathbf{u}|\boldsymbol{\alpha})}{Z(\boldsymbol{\alpha})} = \frac{1}{Z(\boldsymbol{\alpha})} \exp\left(-\frac{\mathcal{L}(\boldsymbol{\alpha} + \mathbf{u}) - \mathcal{L}(\boldsymbol{\alpha})}{\tau}\right), \tag{5}$$

where $\widetilde{p}(\mathbf{u}|\boldsymbol{\alpha}) = \exp\left(-[\mathcal{L}(\boldsymbol{\alpha} + \mathbf{u}) - \mathcal{L}(\boldsymbol{\alpha})]/\tau\right)$ is an unnormalized exponential distribution, and $Z(\boldsymbol{\alpha}) = \int \widetilde{p}(\mathbf{u}|\boldsymbol{\alpha}) \mathrm{d}\mathbf{u}$ is its normalization coefficient. τ is a temperature parameter controlling the variance of the distribution.

Table 1: Configuration of three methods used in the ZARTS scheme. The main difference lies in the meaning of function $\phi(\cdot)$: RS follows the traditional gradient estimation algorithms, MGS estimates the update according to the improvement of loss function, while GLD uses direct search. Note that the ZARTS framework is general and can support more configurations besides the listed ones.

Algorithm	**Sampling strategy**	**Update estimation function** $\phi\left(\{\mathbf{u}_i, \boldsymbol{\omega}^*(\boldsymbol{\alpha}_i)\}_{i=1}^N\right)$
ZARTS-RS	$\mathbf{u}_i \sim q(\mathbf{u}\|\boldsymbol{\alpha})$, any spherically symmetric distribution.	$\mathbf{u}^* = -\xi \cdot \frac{\varphi(d)}{2\mu N} \sum_{i=1}^N \left[\mathcal{L}(\boldsymbol{\alpha}+\mu\mathbf{u}_i) - \mathcal{L}(\boldsymbol{\alpha}-\mu\mathbf{u}_i)\right]\mathbf{u}_i$ (Eq. 4)
ZARTS-MGS	$\mathbf{u}_i \sim q(\mathbf{u}\|\boldsymbol{\alpha})$, any proposal distribution.	$\mathbf{u}^* = \sum_{i=1}^N \left[\frac{\widetilde{c}(\mathbf{u}_i\|\boldsymbol{\alpha})}{\sum_{j=1}^N \widetilde{c}(\mathbf{u_j}\|\boldsymbol{\alpha})}\mathbf{u}_i\right]$ (Eq. 8)
ZARTS-GLD	$\mathbf{u}_i \sim \mathbb{S}^{d-1}$, a uniform distribution on a unit sphere.	$\mathbf{u}^* = \arg\min_i \{\mathcal{L}(\hat{\boldsymbol{\alpha}})\|\hat{\boldsymbol{\alpha}} = \boldsymbol{\alpha}, \hat{\boldsymbol{\alpha}} = \boldsymbol{\alpha} + \mathbf{u}_i\}$ (Eq. 10)

Intuitively, $\mathbf{u}$ with higher probability contributes more to the objective. Hence, the optimal update of architecture parameters can be estimated by $\mathbf{u}^* = \mathbb{E}_{\mathbf{u}\sim p(\mathbf{u}|\boldsymbol{\alpha})}[\mathbf{u}]$. However, since the probability $p(\mathbf{u}|\boldsymbol{\alpha})$ is an implicit function relying on $\mathcal{L}(\boldsymbol{\alpha}+\mathbf{u})$, making it impractical to obtain the expectation, we refer to [32] and apply importance sampling to sample from a proposal distribution $q(\mathbf{u}|\boldsymbol{\alpha})$ with known probability function:

$$\begin{aligned}\mathbf{u}^* = \mathbb{E}_{\mathbf{u}\sim p(\mathbf{u}|\boldsymbol{\alpha})}[\mathbf{u}] &= \int \frac{\tilde{p}(\mathbf{u}|\boldsymbol{\alpha})}{Z(\boldsymbol{\alpha})}\mathbf{u}\mathrm{d}\mathbf{u} = \int q(\mathbf{u}|\boldsymbol{\alpha})\left[\frac{\tilde{p}(\mathbf{u}|\boldsymbol{\alpha})}{Z(\boldsymbol{\alpha})q(\mathbf{u}|\boldsymbol{\alpha})}\mathbf{u}\right]\mathrm{d}\mathbf{u} \\ &= \mathbb{E}_{\mathbf{u}\sim q(\mathbf{u}|\boldsymbol{\alpha})}\left[\frac{\tilde{p}(\mathbf{u}|\boldsymbol{\alpha})}{Z(\boldsymbol{\alpha})q(\mathbf{u}|\boldsymbol{\alpha})}\mathbf{u}\right] \approx \frac{1}{N}\sum_{i=1}^N\left[\frac{\tilde{p}(\mathbf{u}_i|\boldsymbol{\alpha})}{Z(\boldsymbol{\alpha})q(\mathbf{u}_i|\boldsymbol{\alpha})}\mathbf{u}_i\right] \triangleq \hat{\mathbf{u}}^*,\end{aligned} \tag{6}$$

where $\{\mathbf{u}_i\}_{i=1}^N$ are sampled from the proposal distribution $q(\mathbf{u}|\boldsymbol{\alpha})$. Similarly, the normalization coefficient $Z(\boldsymbol{\alpha})$ can be computed as follows:

$$Z(\boldsymbol{\alpha}) = \int \widetilde{p}(\mathbf{u}|\boldsymbol{\alpha})\mathrm{d}\mathbf{u} \approx \frac{1}{N}\sum_{i=1}^N\left[\frac{\tilde{p}(\mathbf{u}_i|\boldsymbol{\alpha})}{q(\mathbf{u}_i|\boldsymbol{\alpha})}\right]. \tag{7}$$

For convenience, we define a ratio representing the weight on each sample as $\widetilde{c}(\mathbf{u}|\boldsymbol{\alpha}) = \frac{\widetilde{p}(\mathbf{u}|\boldsymbol{\alpha})}{q(\mathbf{u}|\boldsymbol{\alpha})}$. The optimal update for architecture parameters in Eq. 6 can be computed by:

$$\hat{\mathbf{u}}^* = \sum_{i=1}^N\left[\frac{\widetilde{c}(\mathbf{u}_i|\boldsymbol{\alpha})}{\sum_{j=1}^N \widetilde{c}(\mathbf{u}_j|\boldsymbol{\alpha})}\mathbf{u}_i\right] = \sum_{i=1}^N\left[\frac{\frac{\exp(-[\mathcal{L}(\boldsymbol{\alpha}+\mathbf{u}_i)-\mathcal{L}(\boldsymbol{\alpha})]/\tau)}{q(\mathbf{u}_i|\boldsymbol{\alpha})}}{\sum_{j=1}^N \frac{\exp(-[\mathcal{L}(\boldsymbol{\alpha}+\mathbf{u}_j)-\mathcal{L}(\boldsymbol{\alpha})]/\tau)}{q(\mathbf{u}_j|\boldsymbol{\alpha})}}\mathbf{u}_i\right]. \tag{8}$$

Finally, the architecture parameters are updated by $\boldsymbol{\alpha} \leftarrow \boldsymbol{\alpha} + \hat{\mathbf{u}}^*$. Importance sampling diagnostics are conducted to verify the effectiveness of ZARTS-MGS (in the appendix).

4.3 Optimizer III: ZARTS-GLD

Unlike the above two algorithms that estimate gradient or the update for $\boldsymbol{\alpha}$, [12] propose the so-called GradientLess Descent (GLD) algorithm, which falls into the category of truly gradient-free (or direct search) methods. The authors provide solid theoretical proof on the efficacy and efficiency of the GLD algorithm and suggestions on the choice of search radius boundaries. Specifically, they prove that the distance between the optimal minimum and the solution given by GLD is bounded and positively correlated with the condition number of the objective function, where the condition number Q is defined as:

$$Q = \max_{1\le i\le K}\left\{\frac{|\mathcal{L}(\boldsymbol{\alpha}+\Delta_i) - \mathcal{L}(\boldsymbol{\alpha})| \cdot \|\boldsymbol{\alpha}\|}{\|\Delta_i\| \cdot |\mathcal{L}(\boldsymbol{\alpha})|}\right\}. \tag{9}$$

The loss landscape in Fig. 1(b) is pretty flat, implying a low condition number, thus the high efficiency of ZARTS-GLD.

Specifically, at each iteration, with a predefined search radius boundary $[r, R]$, we independently sample candidate updates $\{\mathbf{u}_i\}$ for architecture parameters on spheres with various radii $\{2^{-k}R\}_{k=0}^{\log(R/r)}$ and perform function evaluation at these points. By comparing $\mathcal{L}(\boldsymbol{\alpha})$ and $\{\mathcal{L}(\boldsymbol{\alpha}+\mathbf{u}_i)\}$, $\boldsymbol{\alpha}$ steps to the point with minimum value, or stay at the current point if none of them makes an improvement. The architecture parameters are then updated by $\boldsymbol{\alpha} \leftarrow \boldsymbol{\alpha} + \mathbf{u}^*$.

$$\mathbf{u}^* = \arg\min_i\{\mathcal{L}(\hat{\boldsymbol{\alpha}})|\hat{\boldsymbol{\alpha}} = \boldsymbol{\alpha}, \hat{\boldsymbol{\alpha}} = \boldsymbol{\alpha} + \mathbf{u}_i\} \tag{10}$$

4.4 Connection between DARTS and ZARTS

The similarity between gradient-estimation-based zero-order optimization and SGD builds an essential connection when the objective function is differentiable. For ZARTS-RS, we adopt multi-point estimator to approximate the gradient with a limited bound [23, 2]. Details are put in the supplementary material. Therefore, ZARTS-RS degenerates to second-order DARTS if $\mathcal{L}(\boldsymbol{\alpha})$ is indeed differentiable w.r.t $\boldsymbol{\alpha}$ and the iteration number M is set to 1.

Next, we theoretically show that MGS [32] will degenerate to gradient descent algorithm if the first-order Taylor approximation is applied. Then we analyze the relationship between ZARTS-MGS and DARTS.

Proposition 1. *Assuming that $\mathcal{L}(\boldsymbol{\alpha})$ in Eq. 1 is differentiable w.r.t. $\boldsymbol{\alpha}$, MGS algorithm [32] degenerates to SGD (used in vanilla DARTS) by the first-order Taylor approximation for $\mathcal{L}(\boldsymbol{\alpha})$, i.e., $\mathbf{u}^* \propto -\nabla_{\boldsymbol{\alpha}}\mathcal{L}(\boldsymbol{\alpha})$.*

Proof. Denote $\mathbf{g} \triangleq \nabla_{\boldsymbol{\alpha}}\mathcal{L}(\boldsymbol{\alpha})$ as the gradient of $\mathcal{L}$. The Taylor series of $\mathcal{L}$ at $\boldsymbol{\alpha}$ up to the first order gives $\mathcal{L}(\boldsymbol{\alpha}+\mathbf{u}) - \mathcal{L}(\boldsymbol{\alpha}) \approx \mathbf{u}^\top \mathbf{g}$. Applying it to $p(\mathbf{u}|\boldsymbol{\alpha})$ in Eq. 5 yields:

$$p(\mathbf{u}|\boldsymbol{\alpha}) = \frac{e^{-\mathbf{u}^\top \mathbf{g}/\tau}}{Z(\mathbf{g})},\ Z(\mathbf{g}) = \int_{\|\mathbf{u}\|\leq\varepsilon} e^{-\mathbf{u}^\top \mathbf{g}/\tau} \mathrm{d}\mathbf{u}. \tag{11}$$

Since $\|\mathbf{u}\|$ is constrained within ε to make sure the rationality of first-order Taylor approximation, the optimal update $\mathbf{u}^*$ then becomes:

$$\mathbf{u}^* = \frac{\int_{\|\mathbf{u}\|\leq\varepsilon} \mathbf{u}\cdot e^{-\mathbf{u}^\top \mathbf{g}/\tau}\mathrm{d}\mathbf{u}}{Z(\mathbf{g})} = -\frac{\nabla_{\mathbf{g}} Z(\mathbf{g})}{\tau Z(\boldsymbol{\alpha},\mathbf{g})} = -\frac{1}{\tau}\nabla_{\mathbf{g}} \ln Z(\mathbf{g}). \tag{12}$$

Note that $\mathbf{u}^\top\mathbf{g} = -\|\mathbf{u}\|\|\mathbf{g}\|\cos\eta$, where η is the angle between $\mathbf{u}$ and $\mathbf{g}$. According to the symmetry of integral, $Z(\mathbf{g})$ is determined once $\|\mathbf{g}\|$ is given. Therefore, we can formulate $Z(\mathbf{g})$ as $Z(\|\mathbf{g}\|)$. According to the chain rule:

$$\mathbf{u}^* = -\frac{1}{\tau}\nabla_{\mathbf{g}} \ln Z(\mathbf{g}) = -\frac{1}{\tau}\nabla_{\mathbf{g}} \ln Z(\|\mathbf{g}\|) = -\frac{\nabla_{\|\mathbf{g}\|} Z(\|\mathbf{g}\|)}{\tau Z(\|\mathbf{g}\|)}\nabla_g\|\mathbf{g}\| = -\frac{\nabla_{\|\mathbf{g}\|} Z(\|\mathbf{g}\|)}{\tau Z(\|\mathbf{g}\|)\|\mathbf{g}\|}\mathbf{g}. \tag{13}$$

Since $Z(\|\mathbf{g}\|)$, $\nabla_{\|\mathbf{g}\|}Z(\|\mathbf{g}\|)$, $\|\mathbf{g}\|$ are all scalars, we have

$$\mathbf{u}^* \propto -\mathbf{g} = -\nabla_{\boldsymbol{\alpha}}\mathcal{L}(\boldsymbol{\alpha}) = -\nabla_{\boldsymbol{\alpha}}\mathcal{L}_{val}(\boldsymbol{\omega}^*(\boldsymbol{\alpha}),\boldsymbol{\alpha}). \tag{14}$$

That is, the optimal update $\mathbf{u}^*$ in MGS algorithm shares a common direction with the negative gradient $-\nabla_{\boldsymbol{\alpha}}\mathcal{L}(\boldsymbol{\alpha})$, as used by gradient descent. □

Based on Proposition 1, ZARTS-MGS can be seen as an expansion of DARTS, and it degrades to first-order and second-order DARTS when $\boldsymbol{\omega}^*$ is estimated by $\boldsymbol{\omega}^*_{1st}$ and $\boldsymbol{\omega}^*_{2nd}$, respectively. In general, ZARTS-RS/-MGS can degenerate to DARTS, given the differentiability assumption.

However, unlike DARTS, which has to estimate $\boldsymbol{\omega}^*(\boldsymbol{\alpha})$ by $\boldsymbol{\omega}^*_{1st}$ or $\boldsymbol{\omega}^*_{2nd}$ to satisfy the differentiablity property of $\mathcal{L}_{val}$ and update $\boldsymbol{\alpha}$ by gradient descent algorithm, ZARTS, without such assumptions, can compute $\boldsymbol{\omega}^*(\boldsymbol{\alpha})$ by training network weights $\boldsymbol{\omega}$ for arbitrary numbers of iterations, leading to more robust and effective training for architecture parameters, as shown in the next section.

4.5 Variants and Speedup of ZARTS

ZARTS can be flexibly and seamlessly combined with variants of DARTS for boosting as it can be seen as an expansion of DARTS as analyzed in section 4.4. Here, we derive three variants of ZARTS by combining it with prior works: P-ZARTS based on P-DARTS [7], GZAS based on GDAS [10], and MergeZARTS based on MergeNAS [31]. Implementation details are illustrated in the appendix. These variants can speed up ZARTS twice and reduce the search cost to 0.5 GPU-day. Moreover, GZAS and MergeZARTS also reduce the GPU memory cost during the search process. The performance of these variants is reported in Table 5.

Table 3: Performance on CIFAR. The top reports the accuracy of the best model. The bottom gives the mean of four independent searches as used by [38, 6, 37]. $^{\diamond}$ Reported by [10]. * by [38].

	CIFAR-10	Params (M) ↓	Error (%) ↓	Cost (GPU-days) ↓
best	DARTS (1st) [20]	3.3	3.00	0.4
	DARTS (2nd) [20]	3.4	2.76	1.0
	P-DARTS [7]	3.4	2.50	0.3
	ISTA-NAS [36]	3.3	2.54	0.05
	PR-DARTS [40]	3.4	2.32	0.17
	DARTS- [8]	3.5	2.50	0.4
	ZARTS (ours)	3.5	**2.46**	1.0
average	DARTS(1st) [37]	-	3.38±0.23	0.4
	SGAS (Cri.2) [18]	3.9	2.67±0.21	0.3
	R-DARTS [38]	-	2.95±0.21	1.6
	SDARTS-ADV [6]	3.3	2.61±0.02	1.3
	Amended-DARTS [3]	3.3	2.71±0.09	1.7
	DARTS- [8]	3.5±0.1	2.59±0.08	0.4
	ZARTS (ours)	3.7±0.3	**2.54±0.07**	1.0

	CIFAR-100	Params (M) ↓	Error (%) ↓	Cost (GPU-days) ↓
best	AmoebaNet [26]	3.1	18.93$^{\diamond}$	3150
	PNAS [19]	3.2	19.53$^{\diamond}$	150
	ENAS [25]	4.6	19.43$^{\diamond}$	0.45
	P-DARTS [7]	3.6	17.49	0.3
	GDAS [10]	3.4	18.38$^{\diamond}$	0.2
	ROME [30]	4.4	17.33	0.3
	PR-DARTS [40]	3.4	16.45	0.17
	DARTS- [8]	3.4	17.16	0.4
	ZARTS (ours)	4.0	**15.46**	1.0
average	DARTS [20]	-	20.58±0.44*	0.4
	R-DARTS [38]	-	18.01±0.26*	1.6
	ROME [30]	4.4	17.41±0.12	0.3
	DARTS- [8]	3.3	17.51±0.25	0.4
	ZARTS (ours)	4.1±0.13	**16.29±0.53**	1.0

5 Experiments

We first verify the stability of ZARTS (with three zero-order optimization methods RS, MGS, GLD) on the four popular search spaces of R-DARTS [38] on three datasets including CIFAR-10 [17], CIFAR-100 [17], and SVHN [24]. We then follow Amended-DARTS [3] and empirically evaluate the convergence ability of our method by searching for 200 epochs. Performance trends of the discovered architectures are drawn in Fig. 2(a). Next, we compare with the peer methods on the search space of DARTS [20] to show the efficacy of our method. Finally, we derive three variants of ZARTS with faster search speed by combining ZARTS with the variants of DARTS, showing the flexibility and potential of our ZARTS framework. All the experiments are conducted on NVIDIA 2080Ti. The details of search spaces and experiment settings are given in the appendix.

5.1 Stability Evaluation

The instability issue of DARTS has recently drawn increasing attention. Amended-DARTS [3] shows that after searching by DARTS for 200 epochs, skip-connection gradually dominates the discovered architectures. R-DARTS [38] proposes four search spaces, S1-S4, which amplify the instability of DARTS, as such dominance occurs after only 50 epochs of searching. These studies expose the instability of gradient-based methods. To verify the stability of our method, we search on S1-S4 proposed by R-DARTS and conduct convergence analysis following Amended-DARTS.

Table 2: Test error (%) with DARTS and its variants on S1-S4 search spaces, on CIFAR-10/100 and SVHN. We adopt the same settings as R-DARTS [39]. The best and second best are underlined in boldface and in boldface, respectively.

		DARTS	R-DARTS		DARTS		ZARTS (ours)		
			DP	L2	ES	ADA	RS	MGS	GLD
CIFAR-10	S1	3.84	3.11	2.78	3.01	3.10	2.83	**2.65**	**2.50**
	S2	4.85	3.48	3.31	3.26	3.35	3.35	**3.24**	**3.08**
	S3	3.34	2.93	**2.51**	2.74	2.59	2.59	**2.56**	**2.56**
	S4	7.20	3.58	**3.56**	3.71	4.84	4.90	3.70	**3.52**
CIFAR-100	S1	29.46	25.93	24.25	28.37	24.03	23.64	**23.16**	**23.33**
	S2	26.05	22.30	22.24	23.25	23.52	21.54	**20.91**	**21.13**
	S3	28.90	22.36	23.99	23.73	23.37	22.62	**22.33**	**21.90**
	S4	22.85	22.18	21.94	**21.26**	23.20	23.33	21.31	**21.00**
SVHN	S1	4.58	2.55	4.79	2.72	2.53	**2.40**	2.51	**2.48**
	S2	3.53	2.52	2.51	2.60	2.54	2.52	**2.45**	**2.48**
	S3	3.41	2.49	2.48	2.50	2.50	**2.41**	2.52	**2.44**
	S4	3.05	2.61	2.50	2.51	**2.46**	2.59	**2.48**	2.53

Performance on S1-S4. We first search on the four spaces on CIFAR-10, CIFAR-100, and SVHN. Our evaluation settings are the same as R-DARTS [38]. Four parallel tests are conducted on each benchmark, among which the best is reported in Table 2. We observe that ZARTS achieves outstanding performance with great robustness on 12 benchmarks. All three zero-order algorithms outperform DARTS notably. Even the vanilla zero-order algorithm ZARTS-RS achieves similar robust performance as R-DARTS, which verifies our analysis in Fig. 1, i.e., the coarse estimation $\boldsymbol{\omega}^*_{1st}$ in DARTS distorts the landscape and causes instability. Note that though ZARTS-GLD performs best in Table 2, it falls into the category of direct search methods, requiring

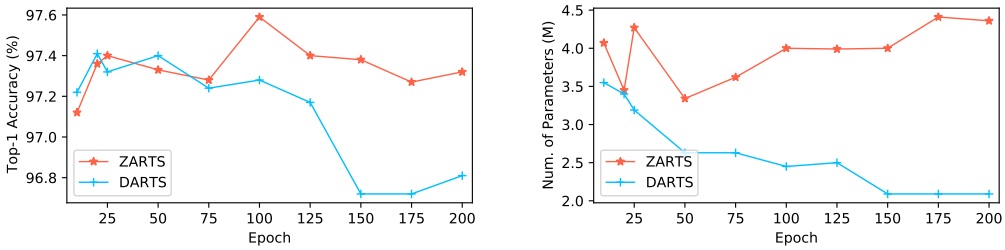

(a) Trend of Top-1 accuracy (b) Trend of Number of Parameters

Figure 2: Trends of accuracy and model size in the search process of DARTS and ZARTS for 200 epochs on CIFAR-10. The top-1 accuracy is obtained by training models for 600 epochs.

more sampling for candidate updates $\mathbf{u}$ and thus more search cost (2.2 GPU-days on the search space of DARTS) than ZARTS-MGS (1.0 GPU-days). ZARTS-MGS is chosen by default if not otherwise specified, considering the trade-off between accuracy and speed.

Convergence Analysis. The convergence ability of NAS methods describes whether a search method can stably discover effective architectures along the search process, i.e., whether the discovered architectures' ultimate performance (top-1 accuracy) can converge to a high value. Amended-DARTS [3] empirically shows that DARTS has a poor convergence ability: accuracy of the supernet increases but the ultimate performance of the searched network drops. Following Amended-DARTS, we run ZARTS and DARTS for 200 epochs and show the trend of performance and number of parameters in Fig. 2. Specifically, we derive one network every 25 epochs during the search process and train each network for 600 epochs to evaluate its ultimate performance. We observe that the networks searched by ZARTS perform stably well (around 97.40% accuracy), while the performance of networks searched by DARTS gradually drops. Moreover, the parameter number of networks searched by DARTS decreases significantly after 50 epochs, indicating that parameterless operations dominate the topology and the instability issue [39] occurs. On the contrary, ZARTS consistently discovers effective networks with about 4.0M parameters, showing the great stability of our method. More details and visualization of architectures are shown in the appendix.

5.2 Performance on the Search Space of DARTS

Results on CIFAR. We conduct four parallel runs by searching with different random seeds and separately training the searched architectures for 600 epochs. The best and average accuracy of four parallel tests are reported in Table 3. In particular, ZARTS achieves 97.46% average accuracy and 97.54% best accuracy on CIFAR-10, outperforming DARTS and its variants. Also, compared with Amended-DARTS that approximates optimal operation weights $\boldsymbol{\omega}^*(\boldsymbol{\alpha})$ by Hessian matrix, our method can stably discover effective architectures in fewer GPU days. Moreover, Table 3 shows our method achieves 83.71% and 84.54% for mean and best accuracy (i.e. 1- error%), on CIFAR-100, outperforming the compared methods by more than 1%.

Table 4: Performance on ImageNet in DARTS's search space by two architectures. † direct search on ImageNet.

Models	**FLOPs** (M) ↓	**Params** (M) ↓	**Top-1 Err.** (%) ↓	**Cost** (GPU-days) ↓
AmoebaNet-A [26]	555	5.1	25.5	3150
NASNet-A [41]	564	5.3	26.0	1800
PNAS [19]	588	5.1	25.8	225
DARTS (2nd) [20]	574	4.7	26.7	1.0
P-DARTS [7]	557	4.9	24.4	0.3
PC-DARTS [35]	586	5.3	25.1	0.1
FairDARTS-B [9]	541	4.8	24.9	0.4
SNAS [33]	522	4.3	27.3	1.5
GDAS [10]	581	5.3	26.0	0.2
SPOS† [13]	323	3.5	25.6	12
ProxylessNAS† [4]	465	7.1	24.9	8.3
Amended-DARTS [3]	586	5.2	24.7	1.7
ZARTS (5.6M params)	647	5.6	**24.3**	1.0
ZARTS (5.0M params)	573	5.0	**24.5**	1.0

Results on ImageNet. For the transferability test, we follow the settings of DARTS to transfer the network discovered on CIFAR-10 to ImageNet. Models are constructed by stacking 14 cells with 48 initial channels. We train 250 epochs with a batch size of 1024 by SGD with a momentum of 0.9 and a base learning rate of 0.5. We utilize the same data pre-processing strategies and auxiliary

classifiers as DARTS. Table 4 shows the performance of our searched networks. ZARTS (5.6M) has 5.6M parameters and achieves 75.7% top-1 accuracy on the validation set of ImageNet, and ZARTS (5.0M) has 5.0M parameters and achieves 75.5% accuracy. Their structure details are given in the appendix, which has fewer skip connection operations than DARTS.

5.3 Variants and Speedup of ZARTS

The results of three variants of ZARTS, including the best and mean performance among four independent searches, are illustrated in Table 5. We search for 50 epochs by each variant and train the discovered architectures for 600 epochs. The search and evaluation settings are introduced in the appendix. Specifically, GZAS outperforms GDAS by 0.3% with similar search cost, only 0.3 GPU-day. P-ZARTS outperforms P-DARTS by 0.15% and even surpasses ZARTS due to the handcrafted criteria in P-DARTS: setting the number of skip connection operations as 2. MergeZARTS achieves state-of-the-art performance with low search cost (0.5 GPU-day). We analyze that the weight merge technique among convolutions in MergeNAS reduces the redundant network weights $\boldsymbol{\omega}$, which alleviates the training difficulty for supernet and thus makes $\boldsymbol{\omega}^*(\boldsymbol{\alpha})$ more accurate after M iterations of gradient descent.

Table 5: We derive the variants of ZARTS by combining ZARTS with the variants of DARTS. Experiments are conducted on CIFAR-10. DARTS, GDAS, and P-DARTS report the best performance in their papers, and MergeNAS reports the average performance.

Models	**Params** (M) ↓	**Error** (%) ↓	**Cost** (GPU-days) ↓	**Memory** (GB) ↓
DARTS (1st) [20]	3.3	3.00	0.4	9.4
DARTS (2nd) [20]	3.4	2.76	1.0	9.4
ZARTS-best (ours)	3.5	**2.46**	1.0	9.4
ZARTS-avg. (ours)	3.7±0.3	**2.54±0.07**	1.0	9.4
GDAS [10]	3.4	2.93	0.2	3.1
GZAS-best (ours)	3.7	**2.58**	0.3	3.1
GZAS-avg. (ours)	3.5±0.2	**2.66±0.07**	0.3	3.1
P-DARTS [7]	3.4	2.50	0.3	9.4
P-ZARTS-best (ours)	3.5	**2.30**	0.4	9.4
P-ZARTS-avg. (ours)	3.3±0.2	**2.41±0.15**	0.4	9.4
MergeNAS (1st) [31]	2.9	2.73±0.02	0.2	4.4
MergeNAS (2nd) [31]	2.9	2.68±0.01	0.6	4.4
MergeZARTS-best (ours)	4.0	**2.19**	0.5	4.4
MergeZARTS-avg. (ours)	3.8±0.2	**2.36±0.18**	0.5	4.4

5.4 Further Discussion

Experimental results verify the efficacy of ZARTS and indicate the advantages of zero-order optimization methods for the NAS task. Nevertheless, this work still has some limitations which can be explored in the future work: i) We adopt three existing zero-order solvers in Table 1, which also suggests new solvers may also be readily reused to improve ZARTS, e.g., in the way of AutoML that automatically determines the suited solver given specific tasks or datasets. In contrast, this feature is not allowed in DARTS as there is little option for the gradient-descent solver. ii) Our experiments focus on classification tasks, while our ZARTS can also search network architectures for more complex tasks. We derive three ZARTS variants from DARTS variants to speed up the search process. GZAS and MergeZARTS can also reduce the GPU memory requirements, making it possible to search on more complex search spaces or tasks, e.g., object detection and segmentation. iii) ZARTS supports to search for the targets whose gradients are intractable or hard to obtain, e.g., FLOPs and latency since ZARTS discards the differentiability assumption and leverages gradient-free algorithms into NAS.

6 Conclusion

DARTS has been a dominant paradigm in NAS, while its instability issue has received increasing attention [3, 38, 6]. In this work, we have empirically shown that the instability issue results from the first-order approximation for optimal network weights and the optimization gap in DARTS, which is also raised in the recent study [3]. To step out of such a bottleneck, this work proposes a robust search framework named ZARTS, allowing for higher-order approximation for $\boldsymbol{\omega}^*(\boldsymbol{\alpha})$ and supporting multiple combinations of zero-order optimization algorithms. Specifically, we adopt three representative methods for experiments and reveal the connection between ZARTS and DARTS. Extensive experiments on various benchmarks show the effectiveness and robustness of ZARTS. To our best knowledge, this is the first work that manages to apply zero-order optimization to one-shot NAS, which provides a promising paradigm to solve the bi-level optimization problem for NAS.

References

[1] Gabriel Bender, Pieter-Jan Kindermans, Barret Zoph, Vijay Vasudevan, and Quoc Le. Understanding and Simplifying One-Shot Architecture Search. In *ICML*, 2018.

[2] Albert S Berahas, Liyuan Cao, Krzysztof Choromanski, and Katya Scheinberg. A theoretical and empirical comparison of gradient approximations in derivative-free optimization. *Foundations of Computational Mathematics*, 2021.

[3] Kaifeng Bi, Changping Hu, Lingxi Xie, Xin Chen, Longhui Wei, and Qi Tian. Stabilizing darts with amended gradient estimation on architectural parameters. *arXiv preprint arXiv:1910.11831*, 2019.

[4] Han Cai, Ligeng Zhu, and Song Han. ProxylessNAS: Direct Neural Architecture Search on Target Task and Hardware. In *ICLR*, 2019.

[5] Pin-Yu Chen, Huan Zhang, Yash Sharma, Jinfeng Yi, and Cho-Jui Hsieh. ZOO: zeroth order optimization based black-box attacks to deep neural networks without training substitute models. In *Proceedings of the 10th ACM Workshop on Artificial Intelligence and Security, AISec@CCS 2017, Dallas, TX, USA, November 3, 2017*, 2017.

[6] Xiangning Chen and Cho-Jui Hsieh. Stabilizing differentiable architecture search via perturbation-based regularization. In *ICML*, 2020.

[7] Xin Chen, Lingxi Xie, Jun Wu, and Qi Tian. Progressive Differentiable Architecture Search: Bridging the Depth Gap between Search and Evaluation. In *ICCV*, 2019.

[8] Xiangxiang Chu, Xiaoxing Wang, Bo Zhang, Shun Lu, Xiaolin Wei, and Junchi Yan. DARTS-: robustly stepping out of performance collapse without indicators. In *ICLR*, 2021.

[9] Xiangxiang Chu, Tianbao Zhou, Bo Zhang, and Jixiang Li. Fair darts: Eliminating unfair advantages in differentiable architecture search. *ECCV*, 2020.

[10] Xuanyi Dong and Yi Yang. Searching for a Robust Neural Architecture in Four GPU Hours. In *CVPR*, 2019.

[11] Abraham D Flaxman, Adam Tauman Kalai, and H Brendan McMahan. Online convex optimization in the bandit setting: gradient descent without a gradient. *arXiv preprint cs/0408007*, 2004.

[12] Daniel Golovin, John Karro, Greg Kochanski, Chansoo Lee, Xingyou Song, and Qiuyi Zhang. Gradientless descent: High-dimensional zeroth-order optimization. In *ICLR*, 2020.

[13] Zichao Guo, Xiangyu Zhang, Haoyuan Mu, Wen Heng, Zechun Liu, Yichen Wei, and Jian Sun. Single Path One-Shot Neural Architecture Search with Uniform Sampling. *arXiv preprint. arXiv:1904.00420*, 2019.

[14] Kaiming He, Xiangyu Zhang, Shaoqing Ren, and Jian Sun. Deep Residual Learning for Image Recognition. In *CVPR*, 2016.

[15] Andrew G Howard, Menglong Zhu, Bo Chen, Dmitry Kalenichenko, Weijun Wang, Tobias Weyand, Marco Andreetto, and Hartwig Adam. Mobilenets: Efficient Convolutional Neural Networks for Mobile Vision Applications. *arXiv preprint. arXiv:1704.04861*, 2017.

[16] Andrew Ilyas, Logan Engstrom, Anish Athalye, and Jessy Lin. Black-box adversarial attacks with limited queries and information. In *ICML*, 2018.

[17] Alex Krizhevsky, Geoffrey Hinton, et al. Learning Multiple Layers of Features from Tiny Images. Technical report, Citeseer, 2009.

[18] Guohao Li, Guocheng Qian, Itzel C Delgadillo, Matthias Müller, Ali Thabet, and Bernard Ghanem. Sgas: Sequential greedy architecture search. In *CVPR*, 2020.

[19] Chenxi Liu, Barret Zoph, Maxim Neumann, Jonathon Shlens, Wei Hua, Li-Jia Li, Li Fei-Fei, Alan Yuille, Jonathan Huang, and Kevin Murphy. Progressive Neural Architecture Search. In *ECCV*, 2018.

[20] Hanxiao Liu, Karen Simonyan, and Yiming Yang. DARTS: Differentiable Architecture Search. In *ICLR*, 2019.

[21] Sijia Liu, Pin-Yu Chen, Bhavya Kailkhura, Gaoyuan Zhang, Alfred O Hero III, and Pramod K Varshney. A primer on zeroth-order optimization in signal processing and machine learning: Principals, recent advances, and applications. *IEEE Signal Processing Magazine*, 2020.

[22] Sijia Liu, Parikshit Ram, Deepak Vijaykeerthy, Djallel Bouneffouf, Gregory Bramble, Horst Samulowitz, Dakuo Wang, Andrew Conn, and Alexander Gray. An ADMM based framework for automl pipeline configuration. In *AAAI*, 2020.

[23] Yurii Nesterov and Vladimir Spokoiny. Random gradient-free minimization of convex functions. *Foundations of Computational Mathematics*, 2017.

[24] Yuval Netzer, Tao Wang, Adam Coates, Alessandro Bissacco, Bo Wu, and Andrew Y. Ng. Reading digits in natural images with unsupervised feature learning. In *NIPSW*, 2011.

[25] Hieu Pham, Melody Y Guan, Barret Zoph, Quoc V Le, and Jeff Dean. Efficient Neural Architecture Search via Parameter Sharing. In *ICML*, 2018.

[26] Esteban Real, Alok Aggarwal, Yanping Huang, and Quoc V Le. Regularized evolution for image classifier architecture search. In *AAAI*, 2019.

[27] Karen Simonyan and Andrew Zisserman. Very deep convolutional networks for large-scale image recognition. *arXiv preprint arXiv:1409.1556*, 2014.

[28] Xingyou Song, Wenbo Gao, Yuxiang Yang, Krzysztof Choromanski, Aldo Pacchiano, and Yunhao Tang. ES-MAML: simple hessian-free meta learning. In *ICLR*, 2020.

[29] Yun-Yun Tsai, Pin-Yu Chen, and Tsung-Yi Ho. Transfer learning without knowing: Reprogramming black-box machine learning models with scarce data and limited resources. *CoRR*, 2020.

[30] Xiaoxing Wang, Xiangxiang Chu, Yuda Fan, Zhexi Zhang, Xiaolin Wei, Junchi Yan, and Xiaokang Yang. ROME: robustifying memory-efficient NAS via topology disentanglement and gradients accumulation. *CoRR*, 2020.

[31] Xiaoxing Wang, Chao Xue, Junchi Yan, Xiaokang Yang, Yonggang Hu, and Kewei Sun. Mergenas: Merge operations into one for differentiable architecture search. In *IJCAI*, 2020.

[32] Sean Welleck and Kyunghyun Cho. Mle-guided parameter search for task loss minimization in neural sequence modeling. *arXiv preprint arXiv:2006.03158*, 2020.

[33] Sirui Xie, Hehui Zheng, Chunxiao Liu, and Liang Lin. SNAS: Stochastic Neural Architecture Search. In *ICLR*, 2019.

[34] Yuhui Xu, Lingxi Xie, Xiaopeng Zhang, Xin Chen, Guo-Jun Qi, Qi Tian, and Hongkai Xiong. PC-DARTS: Partial Channel Connections for Memory-Efficient Architecture Search. In *ICLR*, 2020.

[35] Yuhui Xu, Lingxi Xie, Xiaopeng Zhang, Xin Chen, Guo-Jun Qi, Qi Tian, and Hongkai Xiong. Pc-darts: Partial channel connections for memory-efficient architecture search. In *ICLR*, 2020.

[36] Yibo Yang, Hongyang Li, Shan You, Fei Wang, Chen Qian, and Zhouchen Lin. ISTA-NAS: efficient and consistent neural architecture search by sparse coding. In *NeurIPS*, 2020.

[37] Kaicheng Yu, Christian Sciuto, Martin Jaggi, Claudiu Musat, and Mathieu Salzmann. Evaluating the search phase of neural architecture search. In *ICLR*, 2020.

[38] Arber Zela, Thomas Elsken, Tonmoy Saikia, Yassine Marrakchi, Thomas Brox, and Frank Hutter. Understanding and robustifying differentiable architecture search. In *ICLR*, 2020.

[39] Arber Zela, Thomas Elsken, Tonmoy Saikia, Yassine Marrakchi, Thomas Brox, and Frank Hutter. Understanding and Robustifying Differentiable Architecture Search. In *ICLR*, 2020.

[40] Pan Zhou, Caiming Xiong, Richard Socher, and Steven Chu-Hong Hoi. Theory-inspired path-regularized differential network architecture search. In *NeurIPS*, 2020.

[41] Barret Zoph, Vijay Vasudevan, Jonathon Shlens, and Quoc V Le. Learning Transferable Architectures for Scalable Image Recognition. In *CVPR*, 2018.

Checklist

The checklist follows the references. Please read the checklist guidelines carefully for information on how to answer these questions. For each question, change the default **[TODO]** to [Yes] , [No] , or [N/A] . You are strongly encouraged to include a **justification to your answer**, either by referencing the appropriate section of your paper or providing a brief inline description. For example:

- Did you include the license to the code and datasets? [Yes]
- Did you include the license to the code and datasets? [No] The code and the data are proprietary.
- Did you include the license to the code and datasets? [N/A]

Please do not modify the questions and only use the provided macros for your answers. Note that the Checklist section does not count towards the page limit. In your paper, please delete this instructions block and only keep the Checklist section heading above along with the questions/answers below.

1. For all authors...
   (a) Do the main claims made in the abstract and introduction accurately reflect the paper's contributions and scope? [Yes]
   (b) Did you describe the limitations of your work? [Yes] see Section 5.4.
   (c) Did you discuss any potential negative societal impacts of your work? [N/A]
   (d) Have you read the ethics review guidelines and ensured that your paper conforms to them? [Yes]
2. If you are including theoretical results...
   (a) Did you state the full set of assumptions of all theoretical results? [Yes]
   (b) Did you include complete proofs of all theoretical results? [Yes] See Section 4.4.
3. If you ran experiments...
   (a) Did you include the code, data, and instructions needed to reproduce the main experimental results (either in the supplemental material or as a URL)? [Yes] The codes are included in the supplementary material.
   (b) Did you specify all the training details (e.g., data splits, hyperparameters, how they were chosen)? [Yes] See Section 2.2 and 2.3 in supplementary material.
   (c) Did you report error bars (e.g., with respect to the random seed after running experiments multiple times)? [Yes] The standard deviation of repeated runs is reported.
   (d) Did you include the total amount of compute and the type of resources used (e.g., type of GPUs, internal cluster, or cloud provider)? [Yes] All the experiments are conducted on a single NVIDIA 2080Ti.
4. If you are using existing assets (e.g., code, data, models) or curating/releasing new assets...
   (a) If your work uses existing assets, did you cite the creators? [Yes]
   (b) Did you mention the license of the assets? [Yes]
   (c) Did you include any new assets either in the supplemental material or as a URL? [No]
   (d) Did you discuss whether and how consent was obtained from people whose data you're using/curating? [N/A]
   (e) Did you discuss whether the data you are using/curating contains personally identifiable information or offensive content? [N/A]
5. If you used crowdsourcing or conducted research with human subjects...
   (a) Did you include the full text of instructions given to participants and screenshots, if applicable? [N/A]
   (b) Did you describe any potential participant risks, with links to Institutional Review Board (IRB) approvals, if applicable? [N/A]
   (c) Did you include the estimated hourly wage paid to participants and the total amount spent on participant compensation? [N/A]